J Fluoresc (2006) 16:773–781
DOI 10.1007/s10895-006-0130-8

ORIGINAL PAPER

Fluorescence Recovery Under Decaying Photobleaching Irradiation: Concept and Experiment

Yu. I. Glazachev · V. V. Khramtsov

Received: 30 July 2006 / Accepted: 28 August 2006 / Published online: 27 September 2006

Abstract A novel modification of photobleaching method for measurement of lateral diffusion is developed. In this approach fluorescence recovery kinetics is measured under decaying photobleaching irradiation, termed as fluorescence recovery under decaying photobleaching (FRDP). The time evolution of fluorescence intensity normalized to input irradiation starts from the photobleaching kinetics and transforms into the kinetics of fluorescence recovery at a later stage resulting in appearance of minimum. The analytical solution for the kinetics of fluorescence for Gaussian lineshape of laser beam and hyperbolic decay of irradiation in the first order approximation on bleaching rate was obtained. The accuracy of the analytical function was evaluated with exact numerical solution computed with finite differentiates method. The FRDP method was successfully applied to fluorescein solution in the glycerol/water mixture (80%) under various experimental settings using home-made experimental set-up. The FRDP approach demonstrated 25–30 fold enhancement in signal intensity over classical fluorescence recovery after photobleaching (FRAP) method at 3–5 fold increase in total irradiation. Among other advantages of the FRDP is the opportunity to perform measurements on varying time scales under constant size of the bleaching spot, including "safe" long time measurements. The potential extra advantage of FRDP method for analysis of complex diffusion in the biological system is discussed.

Keywords: Photobleaching · Fluorescence · Diffusion · Fluorescein

Y. I. Glazachev (✉) · V. V. Khramtsov
Institute of Chemical Kinetics and Combustion,
Novosibirsk 630090, Russia
e-mail: glaza@kinetics.nsc.ru

V. V. Khramtsov
Dorothy M. Davis Heart & Lung Research Institute, Division of Pulmonary, Critical Care & Sleep Medicine,
The Ohio State University,
Columbus, OH 43210, USA

Introduction

Fluorescence recovery after photobleaching method (FRAP) is widely used for study of lateral diffusion of the fluorescent probes or endogenous fluorescent compounds in the biological membranes. The classical method, also known as bleach-and-probe approach, is based on the observation of the kinetics of the recovery of integral fluorescence collected from the small spot after partial bleaching of the fluorescent probe with short but intense laser pulse [1]. This method is comparatively simple in realization and interpretation. However, the approach is limited in sensitivity due to the requirement of applying of nonbleaching low-intensive laser irradiation for the probe excitation. In particular, the sensitivity issue becomes critical when studying native cell membranes where the incorporation of exogenous fluorescent probe is strongly restricted. A low signal-to-noise ratio (SNR) also limits analysis of multicomponent or anomalous diffusion [2–5].

Another method, an observation of fluorescence under continuous photobleaching (CP), bleach-probe approach, results in significant increase in SNR. This approach was recently used in combination with other techniques [6, 7] but it has its own limitations. Continuous irradiation causes permanent bleaching and heating of the sample and, therefore, limits long time measurements. In addition, the fluorescence kinetics shows less-informative logarithmic like decay

which complicates quantitative analysis, particularly in case of complex diffusion.

In this paper we present a new modification of fluorescence photobleaching method that can be considered as compiling of bleach-and-probe and continuous bleach-probe approaches. In this method the applied irradiation is significantly higher then merely exciting but decays with time course down to about nonbleaching level. As a consequence, the time evolution of fluorescence intensity normalized to input fluorescence starts from the kinetics of photobleaching and transforms into the kinetics of fluorescence recovery at a later stage resulting in appearance of minimum. The approach gains both an increase in SNR and allowing long time measurements.

Materials and methods

Instrumentation

The experimental setup was constructed on the base of argon laser with wavelength 488 nm and fluorescence microscope. Output irradiation control is provided by the electro-optical modulator (EOM) mounted on the laser unit. The beam after modulator goes through 1 mm diaphragm and then through the piece of glass which reflects part of irradiation into photodiode (PD). The specially designed electronic scheme provides the feedback between the voltage on EOM and reverse current of PD. The required current of PD (which is proportional to output intensity of laser irradiation) is set by compensative scheme with 12-bit digital-analogue-converter (DAC). The PD was used below of its saturation and provided high linearity.

In the present setup the EOM provides 50-fold change of irradiation intensity. In the experiments the 10–12 fold variations in the intensity were applied. After modulator assembly the intensity of irradiation was additionally adjusted with rotating polarizer used as tunable attenuator.

The sampling time was controlled by 24-bit programmable timer. The photomultiplier (PMT) was used in photon counter regime. The DAC, timer and photon counter were controlled and synchronized by microprocessor-based controller connected to computer.

Testing the linearity of photomultiplier

The presented approach requires the linearity of PMT signal versus input irradiation in the wide range. Figure 1 shows a typical dependence of PMT signal of sample fluorescence versus laser irradiation in the absence of photobleaching. The nonbleaching conditions keeping the same fluorescence intensity were achieved by increasing fluorescein concentration with decreasing irradiation intensity and/or defocusing of irradiation beam.

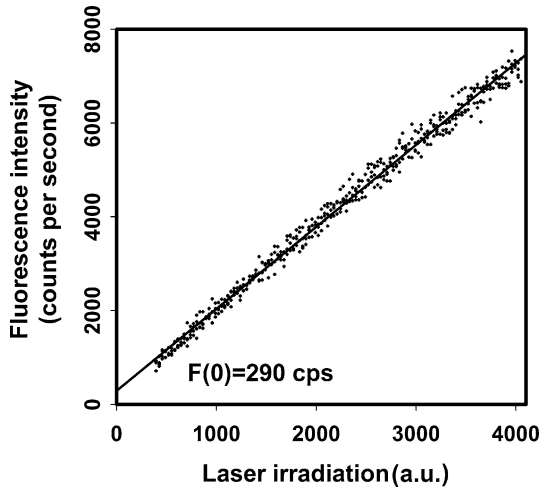

Fig. 1 The dependence of PMT signal of fluorescence of fluorescein solution versus input laser irradiation in the absence of photobleaching. Sampling time is 100 ms with four data point of signal at one value of irradiation intensity. Range of intensity of irradiation is about 400–4000 a.u. (12-bit data of DAC). Data are fitted with linear regression. The calculated value of intercept is 290 ± 10 cps

The 10-fold range of irradiation corresponds to the condition for single experiment. Linear fitting demonstrates a reasonable agreement but with non-zero intercept of about 290 counts per seconds (cps). The non-zero intercept originates from the background signal (a few cps in our set-up) and from non-ideal linearity (small local curvature). The latter effect results in the dependence of intercept value on the range of fluorescence intensity. The tuning of the experimental set-up to eliminate both of these effects could be difficult. However the intercept can be easily taken into account in data analysis describing the observed signal intensity of PMT by the following equation:

$$S(t) = F(t) + bg \tag{1}$$

where F is fluorescence intensity; bg is "background signal" which is time independent but might depend on fluorescence intensity range.

Sample preparation

Fluorescein, sodium salt, was dissolved in 80% glycerol/water mixture to final concentration about 1 μm. The probe solution, about 5 μl, was placed between sample glass and cover glass and sealed up with paraffin. The sample thickness was about 10 μm. Diameter of bleaching/exciting spot was about 5 μm; objective 20 $\times$, numeric aperture 0.65. All measurements were made at room temperature.

Theory

General solution

The time evolution of fluorophore concentration profile under photobleaching irradiation is described by the following equation:

$$\frac{dC(r,t)}{dt} - D\frac{1}{r}\frac{d}{dr}r\frac{d}{dr}C(r,t) = -kI_0C(r,t)I(r,t) \qquad (2)$$

where $C(r,t)$ is two dimensional concentration of fluorophore; $I(r,t) = I(r) \times T(t)$ is time dependent profile of the laser beam, the product of the radial $I(r)$, and temporal, $T(t)$, functions; I_0 is initial integral intensity of irradiation; k is efficiency of photobleaching; D is diffusion coefficient.

The left part of Eq. (2) is derived from classical Smoluchowsky equation for 2D-diffusion with radial symmetry. The right part describes the chemical reaction of photobleaching in the assumptions of single photon reaction and first order on fluorophore concentration. The latter assumption is fulfilled for the fluorescein probe due to predominant oxygen-dependent mechanism of its photobleaching under normal oxygen tension [8, 9]. In general, the deviation from the assumption of the first order of photobleaching takes place when the reaction with the bleaching agent (e.g. oxygen) is significantly slower than reaction between exited fluorophore molecules, termed as dye-to-dye mechanism. The latter situation was observed with fluorescein derivative probe in oxygen free samples [10]. In most physiological conditions, the assumption of the first order of photobleaching should be valid for the common fluorescent probes.

The Eq. (2) can be evaluated in the approximation of low rate of photobleaching and Gaussian shape of laser beam (see Appendix A, Eq. (A5)). The resulted fluorescence normalized to input irradiation for the first order of approximation (see Appendix, Eq. (A6)) is

$$f(t) = \frac{F(t)}{T(t)} = f(0)\left(1 - \frac{kI_0}{\pi r_0^2}\int_0^t \frac{T(x)}{1 + \frac{t-x}{t_D}}dx\right) \qquad (3)$$

where $t_D = r_0^2/4D$ is the characteristic diffusion time.

The term $\frac{kI_0}{\pi r_0^2} = B$ is the slope of $f(t)/f(0)$ at zero time (under condition of $T(0) = 1$). It reflects the integral rate of photobleaching that is independent on diffusion. In general case, the value of initial slope depends on the integral irradiation intensity, radius and the shape of laser beam (see Eq. (A8)).

The further evaluation of Eq. (3) requires to define the decay function of laser irradiation, $T(t)$. Conceptually, this function should decay reasonably fast at the initial stage and slow enough at the later stage. To fit these requirements we used the function of hyperbolic decay as temporal term of irradiation intensity

$$T(t) = \frac{1}{1 + t/t_B} \qquad (5)$$

which gives the analytical solution of Eq. (3) for the kinetics of normalized fluorescence:

$$f(t) = f(0)\left(1 - B\frac{t_B t_D}{t_B + t_D + t}\left\{\ln\left|1 + \frac{t}{t_B}\right| + \ln\left|1 + \frac{t}{t_D}\right|\right\}\right) \qquad (6)$$

where t_B is the characteristic decay time of photobleaching.

Taking into account "background signal" of the PMT (see Eq. (1)), the experimentally measured normalized fluorescence is described by the equation:

$$f(t)_{\text{observed}} = \frac{S(t)}{T(t)} = \frac{F(t) + bg}{T(t)} = f(t) + \frac{bg}{T(t)} = f(t) + bg\left(1 + \frac{t}{t_B}\right) \qquad (7)$$

As one can see the observed normalized fluorescence is a superposition of Eq. (6) and additional term which linearly depends on time and does not interfere with the function $f(t)$. Therefore, the Eq. (7) was employed further for experimental data fitting using bg as additional variable parameter.

Results

Numeric calculations with finite differentiates method

To evaluate the accuracy of Eq. (6) the numerical solutions of Eq. (2) obtained with finite differentiates method (FDM) were computed (see Appendix B).

Figure 2 shows computed normalized fluorescence kinetics fitted with analytical functions Eq. (6) for the bleaching rates corresponding to bleaching depths from 10 to 50%. The calculated curves are presented for two set of parameters: varying diffusion times at constant bleaching rate (Fig. 2a); varying bleaching rates at constant diffusion time (Fig. 2b).

The parameters obtained from the fitting are given in the Table 1. The values of t_D deviate from the original ones within the range from 10 to 30%. The deviation of B is slightly more significant being in the range from 10 to 40%.

The above deviations contribute to the absolute errors that, in particular for calculation of the diffusion coefficient, $D = r_0^2/4tD$, are also strongly affected by inaccuracy in determination of geometric parameters of beam. More important is differential error, which for t_D and, therefore, for

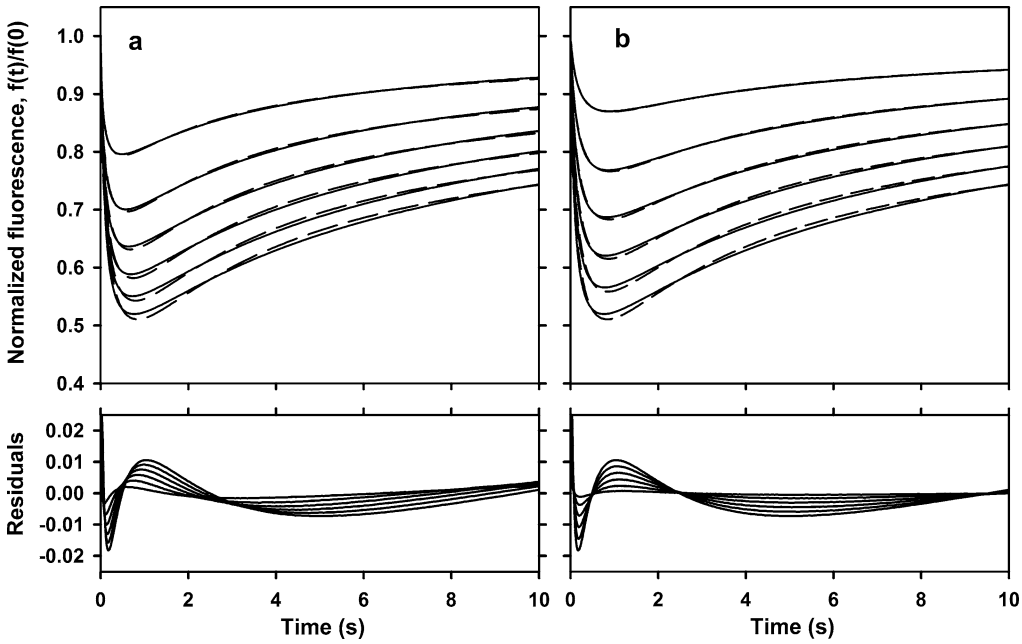

Fig. 2 Functions of normalized fluorescence computed with finite differentiates method (FDM) fitted with analytical solution, Eq. (6). Set of parameters is taken as: $t_B = 1$ s, total time is 10 s, point number is 256, the increasing time step is applied according to Eq. (9) with initial value equal to 9.4 ms. (a) Constant bleaching rate, $B = 6$ s^{-1}, and different diffusion time, $t_D = 1/60,\ 2/60 \cdots 6/60$ s; (b) $t_D = 1/10$ s and $B = 1,\ 2 \cdots 6$ s^{-1}. The parameters obtained from the fitting are presented in the Table 1

D, is within 20% for the mentioned bleaching depths. And if we take, for example, 30% of bleaching depth as a reference, this error will be within 10%, and, therefore, within reasonable experimental error. As the optimal bleaching depths the range from 30 to 40% can be proposed.

Experimental measurements with constant sampling time

Figure 3a shows temporal profile of user-defined input irradiation and the experimental kinetics of observed fluorescence measured for fluorescein solution in the glycerol/water mixture (80% w/w, see Materials and Method). The diffusion under these conditions represents two dimensional projection of three dimensional diffusion which obeys the classical behavior described by Eq. (2). The ratio of the fluorescence and input irradiation, a normalized fluorescence, is shown in Fig. 3b. Solid line represents the best fit obtained with Eq. (7) that demonstrates a good agreement of analytical solution and experimental data (see Fig. 3c). Note that the value of the "background signal," $bg = 240 \pm 10$ cps, was found to be close to that obtained by tuning procedure (290 ± 10 cps, see Fig. 1).

Table 1 Results of fitting of computed solution, obtained with FDM, with analytical function, Eq. (6) (Fig. 2)

t_D, ms original	t_D, ms fitting	B, s^{-1} original	B, s^{-1} fitting	Bleaching depth (%)	SD of residual (%)
16.7	14.8	6	5.0	20	0.17
33.3	27.8	–	4.5	30	0.38
50	40.0	–	4.2	36	0.59
66.7	51.5	–	4.0	42	0.80
83.3	62.6	–	3.8	45	1.0
100	73.4	–	3.6	48	1.2
100	93	1	0.90	13	0.074
–	87.3	2	1.63	23	0.25
–	82.7	3	2.24	31	0.46
–	79	4	2.76	38	0.70
–	76	5	3.21	43	0.95
–	73.4	6	3.6	48	1.2

Note. The calculated parameters are presented in compare with original values.

The measurement under decaying irradiation with constant sampling time results in progressive decrease of the signal-to-noise ratio (SNR) for normalized fluorescence as clearly seen in the residual (Fig. 3c). Note that the initial stage of the kinetics and region around its minimum are most informative for the data analysis. The measurement of long tail of the kinetics is necessary for determination of the asymptotic behavior. However it leads to unwanted increase of the weight of this part due to greater number of points.

The above factors can be taken into account by applying corresponding weighting function in calculation of chi-square. The weight of each experimental i-point is reciprocal to the square of its dispersion, σ_i^2. In the assumption that the value of σ_i^2 of observed fluorescence, F_i, can be taken to be proportional to laser intensity, T_i, it is easy to show that the square of dispersion for normalized fluorescence is

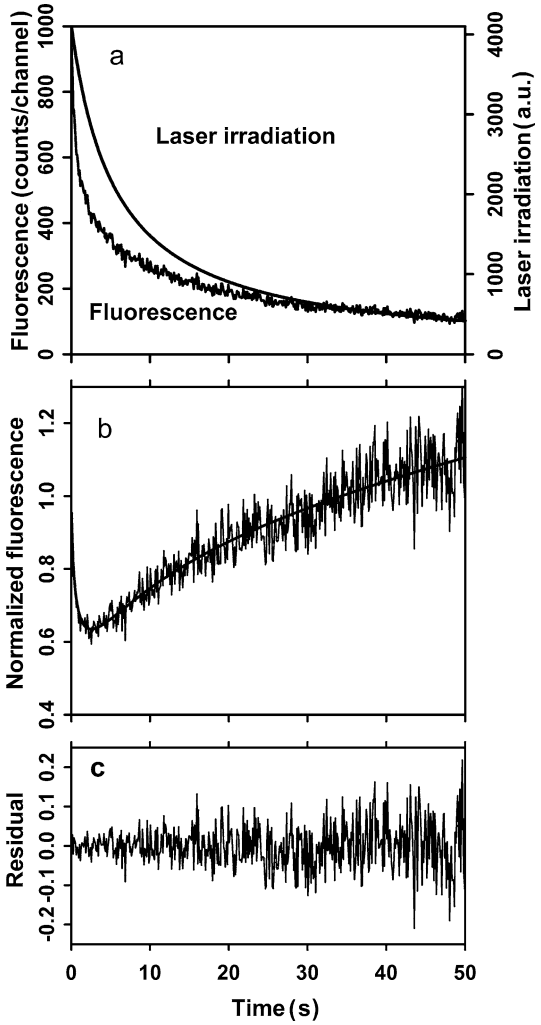

Fig. 3 Experimental data for the fluorescein solution in the glycerol/water mixture measured at room temperature with constant sampling time: (a) temporal profile of input irradiation intensity and kinetics of fluorescence signal intensity; (b) fluorescence intensity normalized to the input irradiation and fitting with Eq. (7) using weight function (see Eq. (8)); (c) residual function which is a difference of experimental and fitting data from (b). Experimental parameters were as following: $t_B = 5.6$ s, $\Delta t = 100$ ms, point number is 512, total time is 51.2 s. Result of fitting: $t_D = 85 \pm 10$ ms, $B = 1.8 \pm 0.2$ s^{-1}, depth is 42%, $bg = 240 \pm 10$ cps, initial intensity is 9.7×10^3 cps

reciprocal to this irradiation intensity. So, the T_i can be used as weighting function in calculation of chi-square for least-square fitting of the normalized fluorescence:

$$\chi^2 = \sum_i T_i \left(\frac{F_i}{T_i} - f(t_i) \right)^2 \tag{8}$$

Experimental measurements with increasing sampling time

As it was mentioned above the most informative part of the kinetics is located in the initial stage at maximum of its slope whereas slowly decaying tail is less informative. For such kinetics it is reasonable to perform the measurements with increasing sampling time. We employed the value of sampling time, Δt, at each i-timestep to be reciprocal to irradiation intensity:

$$\Delta t_i \propto 1/T_i \tag{9}$$

In other words, the decrease in irradiation and, therefore, fluorescence intensity is proportionally compensated by increasing sampling time. While the photomultiplier works as photon counter, the observed signal, S_i, is equal to the intensity of fluorescence multiplied by sampling time (equal to the value of time step). Under these conditions the observed signal is proportional to normalized fluorescence:

$$S_i \propto F_i \Delta t_i \propto F_i / T_i \propto f_i \tag{10}$$

As a consequence, the observed SNR should be practically constant over the kinetics due to the proportionality of the square of signal dispersion, σ_i^2, to the term $F_i \Delta t_i$.

According to Eqs. (5) and (9) the experimental time parameters obey the equations:

$$\begin{aligned} &\Delta t_i = \Delta t_{i-1} \alpha = \Delta t_0 \alpha^i \\ &t_i = \Delta t_0 \tfrac{\alpha^i - 1}{\alpha - 1} = t_B(\alpha^i - 1) \\ &\alpha = 1 + \tfrac{\Delta t_0}{t_B} \\ &i = 0..N-1 \end{aligned} \tag{11}$$

Figure 4 shows the observed kinetics of fluorescence signal with increasing sampling time. The time parameters such as t_B and total time are similar to those shown in Fig. 3. Data fittings demonstrated the same values of calculated parameters.

In fact, mathematically these approaches are identical but the kinetics with increasing sampling time is more preferable for data presentation and analysis. First, it demonstrates the predicted constant value of SNR over the kinetics as can be seen on residual (Fig. 4c). Second, it shows more reasonable distribution of data points over kinetics that is more clearly revealed for the data plotted versus channel number (Fig. 4b). As a consequence, it allows to measure in more details the initial most informative part of the kinetics at maximum of its slope without increase in the number of data points. For example, for the kinetics in Figs. 3 and 4 the number of data points are 512 and 256, respectively, while initial sampling time was twice less for the latter case. This benefit arises for long time kinetics when both initial part and long tail have to be measured with reasonable accuracy.

Measurements on different time scales

The FRDP method allows measuring one sample on different time scales without changing the size of the spot. Indeed, the

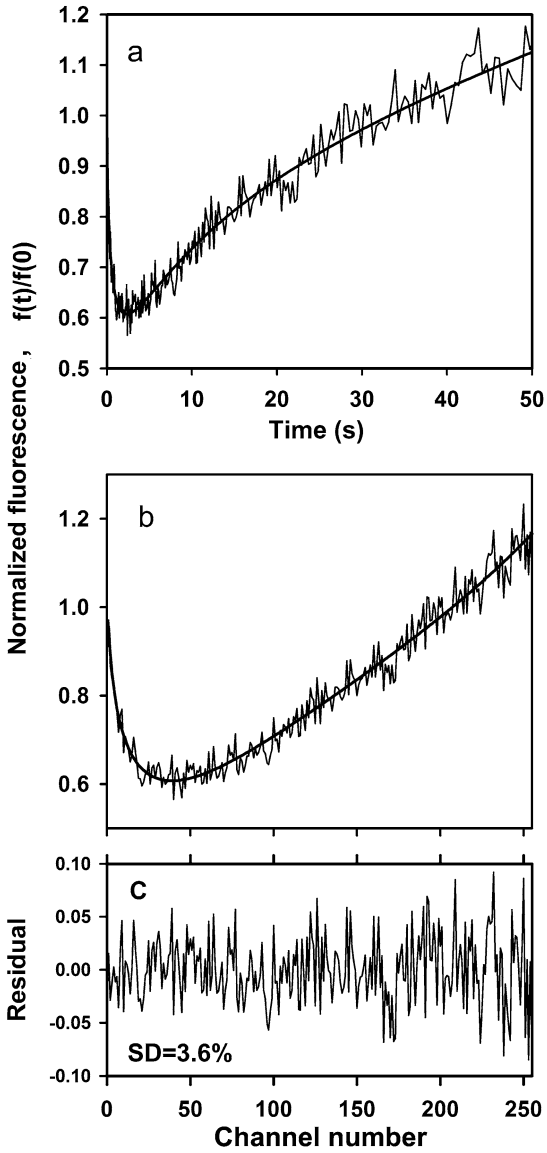

Fig. 4 Experimental kinetics of normalized fluorescence intensity obtained for the fluorescein in the glycerol/water mixture with increasing sampling time: (a) fluorescence intensity versus time; (b) fluorescence intensity versus channel number; (c) residual. Experimental parameters: $t_B = 5.1$ s, $\Delta t_0 = 50$ ms, point number is 256; total time is 56 s. Solid lines is the best fit obtained with Eq. (7) without weight function yielding parameters: $t_D = 82 \pm 10$ ms, $B = 2.0 + 0.2$ s^{-1}, depth is 43%, $bg = 270$ cps , initial intensity is 10^4 cps, SD of residual is 3.6%

value of the characteristic decay time of photobleaching, t_B, can be considered as time scale parameter. Figure 5 shows experimental kinetics measured using different values of t_B in the range from 0.6 s to 5.1 s resulting in total kinetics time from 7 to 56 s. Data fitting yields the same value of t_D within experimental error being equal to about 80 ms.

Decreasing of value of t_B leads to decrease in bleaching depth under constant bleaching rate (Fig. 5a–c). So, to keep this depth at working range it's necessary to increase the bleaching rate and, therefore, the initial intensity of irradiation (Fig. 5d). Note that the sampling time is decreased proportionally to t_B (with constant point number) and, therefore, results in decreasing of the SNR. But on the other hand, the accompanying increasing of irradiation intensity partially compensates the latter effect.

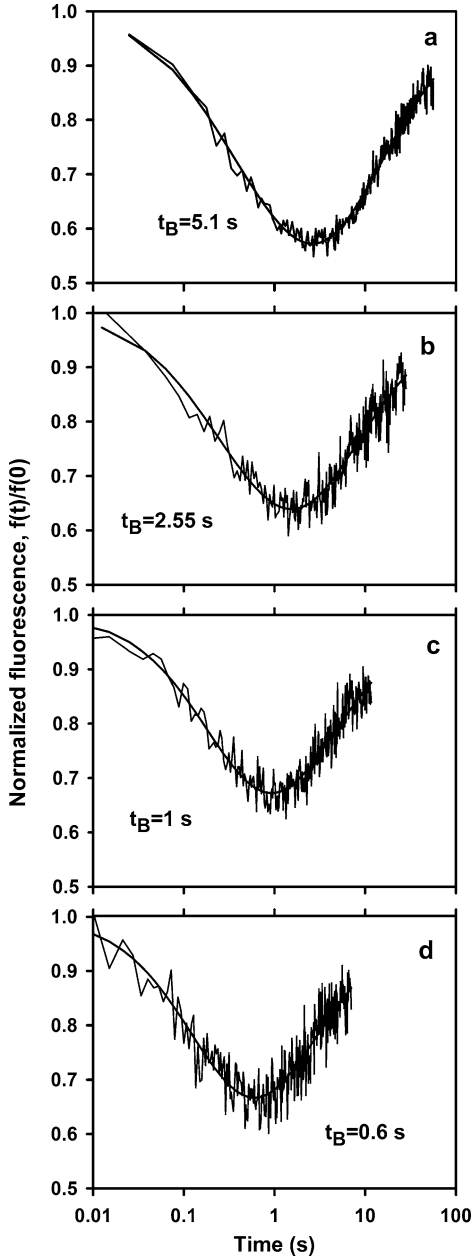

Fig. 5 Experimental data obtained for the fluorescein solution in the glycerol/water mixture with different values of photobleaching decay time, t_B, versus logarithmic time scale. Measurements were performed with increasing sampling time. The data are averaging of 3–4 kinetics with subtracted linear term of "background signals" (see Eq. (7)). The experimental and calculated parameters are: (a) $t_B = 5.1$ s, $\Delta t_0 = 50$ ms, $t_D = 83 \pm 5$ ms, $B = 2.0 \pm 0.1$ s^{-1}, depth is 43%; (b) $t_B = 2.55$ s, $\Delta t_0 = 25$ ms, $t_D = 71 \pm 8$ ms, $B = 2.3 \pm 0.2$ s^{-1}, depth is 36%; (c) $t_B = 1$ s, $\Delta t_0 = 10$ ms, $t_D = 96 \pm 8$ ms, $B = 2.3 \pm 0.2$ s^{-1}, depth is 33%; (d) $t_B = 0.6$ s, $\Delta t_0 = 6$ ms, $t_D = 71 \pm 8$ ms, $B = 3.4 \pm 0.3$ s^{-1}, depth is 33%

Due to symmetry of the appearance of t_D and t_B in Eq. (6) it is possible to measure the samples with different t_D on the same time scale, i.e. t_B. It might be useful for experiments with varied diffusion coefficients but fixed experimental time.

Discussion

We presented a new modification of the method of the recovery of the photobleaching fluorescence. We termed it as fluorescence recovery under decaying photobleaching (FRDP). Now, we would like to discuss the potential advantage of this approach and compare it with other known photobleaching methods.

Figure 6 represents theoretical kinetics calculated in the first order of approximation for CP, FRAP and FRDP methods under the same time settings. For evaluation of these methods the following terms are to be compared: initial fluorescence intensity, which is represented by the value of the bleaching rate, B; signal per channel, proportional to $B \times \Delta t$; overall sample irradiation, proportional to $B \times \int_o^T T(t)dt$ (where T is total time).

For valid comparison the signals should be obtained at the same time scale, point number and constant SNR over the kinetics. In FRAP and CP methods the fluorescence intensity and, therefore, SNR is kept practically constant over the kinetics time scan. Therefore we compared FRAP and

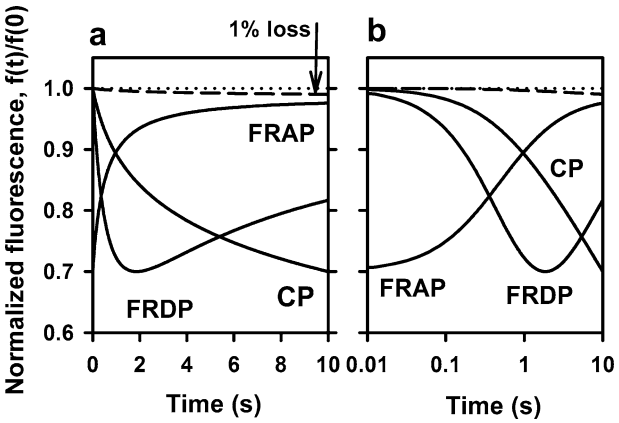

Fig. 6 The calculated kinetics of the fluorescence signal for three photobleaching methods: FRAP, CP and FRDP, versus linear (a) and logarithmic (b) time scales. Set of parameters for all kinetics: total time is 10 s, $t_D = 0.5$ s, $t_B = 1$ s (FRDP only), bleaching depth is 30%, point number is 200, time step for FRAP and CP is 5 ms, increasing time step for FRDP with initial value equal to 1.2 ms. The bleaching rate of exciting irradiation for FRAP is chosen to result in 1% loss of fluorescence due to photobleaching for 10 s (dashed curve). Values of integral bleaching rates, B, under mentioned conditions are 6.6×10^{-3} s^{-1}, 0.20 s^{-1} and 0.78 s^{-1}(initial) for FRAP, CP and FRDP, respectively. Function for CP and dashed curve is $1 - Bt_D \ln(1 - t/t_D)$ with its own set of parameters

Table 2 An increase of the experimental parameters for FRDP and CP methods compared with that for FRAP, obtained for the kinetics shown in Fig. 6

	Initial intensity	Signal per channel	Total irradiation
CP	30	30	5.4
FRDP	120	28	5.1

CP data with the FRDP kinetics obtained with increasing sampling time which also shows constant SNR (Fig. 4). Table 2 shows the results of the corresponding comparison of the experimental parameters of FRDP and CP methods with FRAP.

The obtained results can slightly vary depending on time scale variations. Reasonable average estimations shows 25–30 fold increase of the signal while 3–5 fold increase of total irradiation in the FRDP approach compared with FRAP.

Similar effect for signal intensities for FRDP and CP originates from the same nature of signal enhancement, namely integral irradiations while measurement (equal to overall irradiation for the mentioned methods), which are also the same (see Table 2). In FRAP method the overall total irradiation includes the short intense bleaching pulse that doesn't contribute to signal intensity.

Note two order of magnitude increase in initial intensity of FRDP signal compared with that for FRAP. In our experiments (Figs. 3–5) this value was equal to $(1.0–1.3) \times 10^4$ cps. So, the applying the classical FRAP for our sample will result in about 100 cps for prebleach fluorescence intensity.

The FRDP approach enables measuring the same sample on different time scales only by changing the value of t_B (Fig. 5). In others words, it allows to expand experimentally the most informative part of the kinetics (e.g., in the vicinity of its minimum). This possibility does not have theoretical limitations but the experimental ones only, such as sample size, its time stability, etc. In particularly, it may be very effective in the studies of anomalous diffusion, which is described, in fact, by the dependence of diffusion coefficient on time. Note, that the analysis of anomalous diffusion in FRAP approach requires prolonged kinetics measurement which strongly interferes with another factors (e.g., presence of immobile fraction, slight bleaching by exciting beam) [3, 11, 12].

Another expected benefit of different time scale measurements is the possibility to extract the influence of border while studying small samples. The boundary effect depends on the ratio of the width of bleached fluorophore concentration profile to sample size that, on the other side, can be varied by experimental time settings. It could allow excluding interference with, for example, immobile fraction, which is independent on time scale.

One more potential important advantage of FRDP method can be revealed in the analysis of complex multicomponent

diffusion. Several approaches are used in the analysis of the corresponding kinetics data. Most popular approach is the parametric one, which is applied for the analysis of both multicomponent and anomalous diffusion [2, 3, 5]. Another approach is the computing of distribution of diffusion coefficients, which is a matter of inverse problem solution. The obtained distribution can be further analyzed for the type and contents of diffusion. Periasamy and Verkan [4] successfully applied the maximum entropy method for analysis of both multicomponent and anomalous diffusion in FRAP method. The accuracy of such analysis strongly depends on the kernel (or basic) function, which is monotone for classical FRAP. In the FRDP method such function is represented by Eq. (6) with the minimum that should improve an accuracy of the analysis. The presentation versus logarithmic time scale more clearly demonstrated this advantage (Fig. 6b). Note, that for advanced analysis of FRAP kinetics the logarithmic scale was usually used [2–4].

In conclusion, the control of the irradiation intensity is the exclusive tool of FRDP method. This tool provides enhanced opportunity for the investigator to tune experimental conditions for optimizing data output and providing extra information. The experimental set-up allows specifying any reasonable irradiation function. The observed normalized kinetics for the first order of photobleaching can be calculated either analytically or numerically using Eq. (3), or computed with FDM (Eq. (B2)). In general, the FRDP approach can be evaluated for various shapes of irradiated area, which is applied, for example, in pattern photobleaching techniques [5].

Appendix

Analytical evaluation

In the approximation of low bleaching, i.e. value of k, the Equation (2)! can be reduced to

$$\frac{dC_1(r,t)}{dt} - D\frac{1}{r}\frac{d}{dr}r\frac{d}{dr}C_1(r,t) = -kI_0C_0I(r,t) \tag{A1}$$

In general, the next order of approximations of concentration profile, $C_n(r,t)$, obeys the recurrent equations:

$$\frac{dC_n(r,t)}{dt} - D\frac{1}{r}\frac{d}{dr}r\frac{d}{dr}C_n(r,t) = -kI_0C_{n-1}(r,t)I(r,t) \tag{A2}$$

The concentration profile in Eq. (A2) can be found using following Poisson integral solution [13]:

$$C_n(r,t) = \frac{k\cdot I_o}{D}\int_0^t\int_\xi G(r,t;\xi,\tau)\,C_{n-1}(\xi,\tau) \times I(\xi,\tau)\,d^2\xi d\tau - \frac{1}{D}\int_\xi G(r,t;\xi,0) \times C_{n-1}(\xi,0)\,d^2\xi \tag{A3}$$

where

$$G(r,t;\xi,\tau) = -\frac{1}{4\pi(t-\tau)}\exp\left(-\frac{|r-\xi|^2}{4D(t-\tau)}\right), \quad \text{for } t > t,$$

is Green function for two dimensional diffusion equation.

The observed kinetics of normalized fluorescence is

$$f(t) = \int C(r,t)I(r)d^2r \tag{A4}$$

For the Gaussian shape for laser beam

$$I(r) = \frac{2}{\pi r_0^2}\exp\left(\frac{2r^2}{r_o^2}\right) \tag{A5}$$

Equations (A2)–(A4) can be further evaluated. The resulted normalized fluorescence could be expressed as a series of the following integral functions:

$$\frac{f(t)}{f(0)} = 1 - \frac{kI_0}{\pi r_0^2}\int_0^t \frac{T(x)}{1+\frac{t-x}{t_D}}dx + \left(\frac{kI_0}{\pi r_0^2}\right)^2\int_0^t\int_0^y \frac{T(x)T(y)}{\left(1+\frac{y-x}{t_D}\right)\left(1+\frac{t-y}{t_D}\right)-\frac{1}{4}}dxdy + \cdots \tag{A6}$$

where $t_D = r_0^2/4D$ is characteristic diffusion time.

The Eq. (A6) can be expressed as

$$f(t)/f(0) = 1 - Bg(B,t) = 1 - Bg_1(t) + B^2g_2(t) + \cdots \tag{A7}$$

where B is integral rate of photobleaching.

The value of B obeys the following equation for any shape of beam:

$$B = \frac{1}{f(0)}\left[\frac{df(t)}{dt}\right]_{t=0} = kI_0\int_S I(r)^2dS \tag{A8}$$

The kinetics of fluorescence for immobile fraction for Gaussian beam shape can be found exactly from Eq. (2) putting $D = 0$:

$$f(t)_{imm}/f(0)_{imm} = \frac{1}{K(t)}\left(1-e^{-K(t)}\right) \tag{A9}$$

where

$$K(t) = \frac{2kI_0}{\pi r_0^2} \int_0^t T(x)dx$$

Finite differentiates method

For numerical solution of the equation of diffusion Eq. (2) with finite differentiate method the six-point scheme centered at halfway timestep has been applied. This scheme is called the Crank-Nicholson scheme and is the second-order accurate both in time (τ) and coordinate (h) steps and is unconditionally stable [14].

The resulting recurrent system of linear equations for computing of concentration profile at timestep $m+1$ evaluated for Eq. (2) is

$$\begin{aligned}&\left(\mathrm{E} + \Lambda\mu_m + \left(\mathrm{E}\varphi^m\right)\tau_m/2\right)c^{m+1}\\ &\quad = (\mathrm{E} - \Lambda\mu_m - (\mathrm{E}\varphi^m)\tau_m/2)c^m + \lambda\mu_m \qquad \text{(B1)}\end{aligned}$$

where c^m is column vector of concentration profile at mth timestep; E is unit matrix; Λ is tridiagonal matrix ($\Lambda_{\mathrm{n,n}} = 1$, $\Lambda_{\mathrm{n,n+1}} = -(1 \pm 1/2\mathrm{n})/2$, $\Lambda_{0,1} = -1$); $\tau_m = t_{\mathrm{m}+1} - t_m$ is the value of time step; $\mu_m = D \times \tau_m/h^2$ is dimensionless parameter; λ is column vector with zero elements except the last one, $\lambda_{N-1} = 1 + 1/2(N-1)$; φ^m is column vector of right-side function at timestep $m + 1/2$, i.e. $\varphi^m{}_n = k \times I(r_n, t_{m+1/2})$. The length of column vectors is N, dimension of matrices is $N \times N$, coordinate index range $n = 0..N-1$. Boundary and initial conditions are $c_N^m = c_n^0 = 1$, $dc/dr(r=0) = 0$.

The observed kinetics of normalized fluorescence was obtained by numerical computing of Eq. (A3).

For the solution of simplified equation Eq. (A1) the scheme is reduced to

$$(\mathrm{E} + \Lambda\mu_m)\,c^{m+1} = (\mathrm{E} - \Lambda\mu_m)\,c^m - \varphi^m\tau_m + \lambda\mu_m \qquad \text{(B2)}$$

Computing of Eqs. (B2) and (A3) with Gaussian shape of beam, Eq. (A5), and hyperbolic decay for $T(t)$, Eq. (5), results in numerical solution for normalized fluorescence coinciding with analytical solution, Eq. (6).

References

1. Axelrod D, Koppel DE, Schlessinger J, Elson E, Webb WW (1976) Mobility measurement by analysis of fluorescence photobleaching recovery kinetics. Biophys J 16:1055–1069
2. Gordon GW, Chazotte B, Wang XF, Herman B (1995) Analysis of simulated and experimental fluorescence recovery after photobleaching Data for two diffusing components. Biophys J 68:766–778
3. Feder TJ, Brust-Mascher I, Slattery JP, Baird B, Webb WW (1996) Constrained diffusion or immobile fraction on cell surfaces: a new interpretation. Biophys J 70:2767–2773
4. Periasamy N, Verkman AS (1998) Analysis of fluorophore diffusion by continuous distributions of diffusion coefficients: application to photobleaching measurements of multicomponent and anomalous diffusion. Biophys J 75:557–567
5. Starr TE, Thompson NL (2002) Fluorescence pattern photobleaching recovery for samples with multi-component diffusion. Biophys Chem 80:1575–1584
6. Hagen GM, Roess DA, de Leon GC, Barisas BG (2005) High probe intensity photobleaching measurement of lateral diffusion in cell membranes. J Fluoresc 15:873–882
7. Wachsmuth M, Weidemann T, Muller G, Hoffmann-Rohrer UW, Knoch TA, Waldeck W, Langowski J (2003) Analyzing intracellular binding and diffusion with continuous fluorescence photobleaching. Biophys J 82:1828–1834
8. Song L, Hennink EJ, Young IT, Tanke HJ (1995) Photobleaching kinetics of fluorescein in quantitative fluorescence microscopy. Biophys J 68:2588–2600
9. Song L, Varma CA, Verhoeven JW, Tanke HJ (1996) Influence of the triplet excited state on the photobleaching kinetics of fluorescein in microscopy. Biophys J 70:2959–2968
10. Corbett JD, Cho MR, Golan DE (1994) Deoxygenation affects fluorescence photobleaching recovery measurements of red cell membrane protein lateral mobility. Biophys J 66:25–30
11. Georgiou G, Bahra SS, Mackie AR, Wolfe CA, O'Shea P, Ladha S, Fernandez N, Cherry RJ (2002) Measurement of the lateral diffusion of human MHC class I molecules on HeLa cells by fluorescence recovery after photobleaching using a phycoerythrin probe. Biophys J 82:1828–1834
12. Endress E, Weigelt S, Reents G, Bayerl TM (2005) Derivation of a closed form analytical expression for fluorescence recovery after photo bleaching in the case of continuous bleaching during read out. Eur Phys J E Soft Matter 16:81–87
13. Korn GA, Korn TM (1968) Mathematical handbook, McGraw-Hill Book Company, New York
14. Press WH, Teukolsky SA, Vetterling WT, Flannery BP (1992) Numerical recipes in C. Cambridge University Press, Cambridge